Structure and stability of *p*-cresol – xenon clathrate: Raman spectroscopy study

Maria M. Ilczyszyn[a,*], Marek Ilczyszyn [a], Marcin Selent[a,b]

[a] Faculty of Chemistry University of Wrocław, Poland
[b] NMR Research Unit, Faculty of Science, University of Oulu,90014 Oulu,Finland
[*] Corresponding author
E-mail address: maria.ilczyszyn@chem.uni.wroc.pl

ABSTRACT

Interaction between *p*-cresol and xenon was studied by Raman spectroscopy. The main questions are crystal structure of resulting clathrate and its stability. The most informative regions of our spectra are those related to the O-H stretching vibrations, the aromatic ring vibrations between 900 and 800 cm^{-1} and the lattice vibrations of the host. From obtained data and their analysis we confirmed formation of hexagonal rings of $[\cdots O\text{-}H\cdots O\text{-}]_6$ hydrogen bonds as the main structural motif of the clathrate cages and we estimated length of the O···O bridges of these bonds. We found evidence that the last factor is responsible for low stability of studied complex and for higher stability of similar clathrates formed by hydroquinone.

1. Introduction

Xenon atoms are peculiar participants in interactions with different atoms, molecules and molecular systems due to their properties: the big electron cloud, extreme hardness and high electronegativity [1]. In some cases stable chemical compounds are formed by xenon but in most cases its interactions are very weak and reversible. Both these categories gather great attention: stable xenon compounds constitute new materials [2,3], very weak interactions in unstable complexes may illustrate processes playing an important role in human body (anesthesia in the first [4-8]) and generally in nature (astrochemistry for example [9,10]).

Anesthesia is caused by many chemical species of different molecular structure and physicochemical properties and the most important and common feature of these species is their ability to very weak and reversible interactions [11]. Anesthetic agents applied in medical area should additionally meet several requirements – non-toxicity in the first. Xenon

gas perfectly meets these conditions and appears as an excellent anesthetics [4-8]. For this we are interested in studies of very weak molecular interactions with its participation [12-18].

Useful models for studying this kind of phenomena are some clathrates with Xe as the guest. For example phenol and some substituted phenols form stable crystal structures at right temperature with cavities occupied by xenon engaged in very weak interactions with the cage components [19-21]. Recently we have studied hydroquinone – Xe clathrate and we have found evidence on Xe – acidic proton H-bonding-like interactions in the cavities formed by hexagonal rings of coupled $[\text{-O-H}\cdots\text{O-}]_6$ hydrogen bonds [12,13]. Similar structural motif is expected in clathrates formed by some phenol derivatives with Xe [19-22]. Also the *p*-cresol – Xe clathrate is expected to be structurally similar to these systems [19,20].

p-Cresol – Xe crystal (PCXe) is unstable at room temperature and under standard pressure of xenon gas. For this only scarce information on its physical and chemical properties can be found in scientific literature [19,20,23-25]. Instability of PCXe hinders determination its crystal structure by diffraction methods. Since of this X-ray diffraction structure of PCXe does not exist and only some suggestions are available in the literature [19,20,24]. In such case indirect methods for structure determination can be considered instead of complicated methods of XRD measurements at high pressures and/or at low temperatures (for example powder X-ray diffraction measurements for noble gas hydrates [26,27]).

In this article we present our consideration on structure of unstable PCXe crystal based on the Raman spectra of *p*-cresol (PC) and PCXe crystals measured by us and by taking into account: (i) crystal structures of other structurally similar but more stable clathrates [12,13,19,20] and (ii) theoretical prediction of crystal structure of unstable clathrates of xenon with F-substituted phenols and crosschecked by ^{129}Xe NMR experiment [22].

Recently different clathrates of hydroquinone have been studied using vibrational methods but in these cases bands due to guests vibrations were recorded and considered [28-30]. Unfortunately this kind of useful information is unavailable in the case of xenon clathrates.

Here we intend to show utility of Raman spectroscopy in structural studies on unstable PCXe molecular system for which determination of the crystal structure by X-ray diffraction methods is very difficult. Raman spectroscopy, similarly as infrared spectroscopy, is excellent tool for the detection of intermolecular interactions of different strength, their variations and formation of new species. From Raman band positions, their changes and their number one can easily recognize whether new complex/species is formed and which structural elements

are involved in the complex formation. In turn this information can be very useful in determining the structure of new species. In our studies we pay special attention on the H-bonding systems as expected main constituents of considered clathrates.

2. Experimental

Commercially available *p*-cresol (Sigma-Aldrich, purity ≥99%) was used without additional purification. Two its samples were prepared in pyrex glass tubes (4 mm outer diameter, 0.8 mm walls) and next connected to a volume-calibrated vacuum line. The first one was then flame sealed after a short evacuation of the air. To the second tube xenon gas (Chemgas) was additionally transferred and its amount was controlled by the pressure drop in the vacuum line, measured with a digital pressure gauge (1 hPa precision). Finally this tube was also flame sealed when the gas pressure was equal to $3x10^4$ hPa. Both samples were kept for at least two weeks at ca. 273 K prior to the Raman measurements.

The Raman spectra of *p*-cresol (PC) and *p*-cresol with xenon (PCXe) samples were recorded at 298, 200, 150 and 100 K temperatures and over the wavenumber range of 3600-25 cm^{-1} with resolution 2 cm^{-1}, with a Jobin-Yvon Ramanor U 1000 spectrometer equipped with CCD and photomultiplier detectors. The GEM 532 nm laser (diode-pumped solid-state laser) was used for excitation with a power at the sample of about 100 mW. The temperature was maintained by a SI-9700-1 temperature controller and a closed cycle helium cryostat (ARS Displex Model CS202-X1.Al closed cycle cryostat).

No digital processing operations were applied to the recorded Raman spectra. The wavenumbers of the bands gathered in Table 1 were taken directly from the Raman spectra. The program GRAMS/386 Galactic Industries was used for determination of intensities of chosen Raman bands (846 and 824 cm^{-1}; 844 and 822 cm^{-1})

3. Results and discussion

3.1 Raman spectra of PC and PCXe

The Raman spectra of PC and PCXe crystalline samples at room temperature are shown in Figs 1. The spectra of PCXe at 100, 150, 200 and 298 K temperatures are presented in supplementary material (Figs S1, S2, S3). The wavenumbers of the bands at room

temperature, and their proposed assignments, are summarized in Table 1. The band assignments given in the last column of Table 1 are based on the theoretical predictions of the internal vibrations of *p*-cresol [31], on the comparison of our assignment to the assignment proposed for tyrosyl residues in proteins [32] and to the Raman active lattice vibrations of aromatic organic compounds [33]. The wavenumbers of the bands observed in the temperature dependent Raman spectra of PCXe are collected in Table S1 (supplementary material).

Below we consider: (i) four regions of the Raman spectra and relations between the bands recognized by us in these spectra, (ii) known crystal structures of PC molecular system and (iii) expected structure of PCXe molecular system. One should note that revised detailed crystal structure of PC at 173 K was published in 2015 [34]. In this report two crystal forms of PC are presented: stable I (the monoclinic space group $P2_1/n$) and metastable II (the monoclinic space group $C2/c$) [34]. Their melting points are 308 and 309 K, respectively. In the case of PCXe only some suggestions related to its crystal structure are available [19,20,24]. Trofimov and Kazankin obtained this clathrate for the first time – it was done at room temperature and under 10^4 - $2x10^4$ hPa pressure of the gas ($3x10^4$ hPa in our study) [24].

3.1.1 O-H stretching vibrations

Two very weak bands in the spectrum of PC at 3320 and 3224 cm^{-1} are assigned to the ν(OH) stretching vibrations (Table 1, Fig. 1a). The number of bands and their positions are in good qualitative agreement with the most stable structure I of PC crystal [34]. In this case, Báthori et al. [33] have predicted two kinds of the O-H···O bonds of different H-bridge distances: R(O···O) = 2.719 Å and R(O···O) = 2.673 Å. Taking into account well known Novak relationship between ν(OH) wavenumber and R(O···O) distance for O-H···O bonds [35] the bands observed in our Raman spectrum were assigned as follows: the band at 3320 cm^{-1} to the longer H-bond and band at 3224 cm^{-1} to the shorter H-bond (Table 1, Fig. 1a). One should also note that these two H-bonds are bent (134.1° and 153.8°, respectively) and for this reason they are probably weaker then corresponding straight line ones.

Metastable form II of PC crystal consists of three different and much more linear O-H···O bonds: R(O···O) = 2.674, 2.656 and 2.630 Å [34]. These H-bonds are not reflected in our Raman spectrum of PC (Table 1, Fig. 1a). We conclude that only structure I is formed in our PC sample.

Considered region of the Raman spectrum becomes simpler by inserting Xe to the *p*-cresol sample. In the PCXe spectrum only one ν(OH) band at 3224 cm^{-1} is observed (Table 1, Fig. 1a). It reveals an active role of Xe atoms, the PC structure variation due to the Xe gas and formation of uniform H-bonds in the PCXe sample.

On cooling the band due to the ν(OH) vibration of PCXe slightly shifts to lower wavenumber from 3224 cm^{-1} at 298 K to 3197 cm^{-1} at 100 K (Table S1). This finding indicates that the O-H···O hydrogen bonds of the clathrate cages become stronger at lower temperatures [35].

3.1.2 C-H stretching vibrations

The bands due to the C-H stretching vibrations of the aromatic ring are identified in the 3100 - 3000 cm^{-1} region of Raman spectrum of PC. Their positions are at 3058, 3042 and 3010 cm^{-1}. When the *p*-cresol crystals are saturated with xenon gas the corresponding bands shift slightly to 3060, 3039 and 3013 cm^{-1}, respectively in the Raman spectrum of PCXe (Table 1, Fig. 1a).

The symmetric stretching vibration of the $–CH_3$ group is observed at 2923 cm^{-1} in the spectrum of PC. When p-cresol is saturated with xenon gas the corresponding band is localized at 2920 cm^{-1}. The bands due to the asymmetric stretching vibrations of the $–CH_3$ group are identified at 2951 cm^{-1} (shoulder) and at 2868 cm^{-1} (weak band) in the Raman spectrum of PC. Their counterparts in the spectrum of PCXe are slightly shifted to lower wavenumbers and are observed at 2950 and 2865 cm^{-1}, respectively.

Similar observations related to the stretching vibrations of the methyl group of PC were reported by Khriachtchev et al [23]. They studied *p*-cresol and *p*-cresol with Xe using infrared spectroscopy of a low temperature Ne matrixes and quantum mechanical calculations. Two kinds of interactions with the Xe participation were found by them: to the π electron system and also to the hydroxyl group of PC (the H-bonding-like interaction). They concluded that considered variations of the stretching vibrations of the $–CH_3$ group result from these interactions [23].

3.1.3 Vibrations in 900 – 800 cm^{-1} region

In this region of our Raman spectra of PC and PCXe we have found a doublet bands resulting from Fermi resonance between ν_1 (the ring-breathing vibrations of the aromatic ring)

and ν_{16a} (the out-of-plane ring-bending vibrations of the aromatic ring) vibrations (Tables 1, 2, Fig. 1c). This kind of doublet was previously recognized by Siamwiza et al. [32] in Raman spectra of tyrosine residues in proteins and in the spectra of several model compounds. They have shown that this doublet is very sensitive on a state of the tyrosine hydroxyl group, especially on H-bonding to this group. The intensity of the doublet component at higher wavenumber (component 1) is higher for a weak H-bonding and the situation turns when the O-H distance increases (H-bonding becomes stronger) [32].

Table 2 presents the positions and the intensity ratios of this doublet in our Raman spectra of PC and PCXe. These results show that the hydroxyl groups in both samples are non-ionized and that the H-bond in PCXe is stronger then corresponding bonds in PC. This conclusion agrees with the positions of the νOH bands in Raman spectra of PC and PCXe (Table 1): 3320, 3224 cm^{-1} and 3224 cm^{-1}, respectively, where the higher wavenumber indicates the weaker O-H···O bond [35].

3.1.4 Lattice vibrations

Raman spectra of PC and PCXe are substantially different in the region of the lattice vibrations, 150 – 25 cm^{-1}, in which rotational vibrations of *p*-cresol molecules in the crystal are expected (Table 1, Fig. 1d). The most important feature seems to be the reduction of number of bands when PC is converted into PCXe. The positions of the bands in this spectral region are also different.

These observations can be related to three possibilities: (i) *p*-cresol molecules are uniform in the crystal structure of PCXe while in the PC structure I two different kinds of these molecules are present [34]; (ii) rotation of *p*-cresol molecules in PCXe crystal is more restricted; (iii) the selection rules for rotational modes in both crystals are different. Below this last expectation is considered in details.

As follows from XRD data *p*-cresol crystallizes in the $C_{2h}^5 = P2_1/n$ ($P2_1/c$) space group of monoclinic system, Z=4 [34,36]. An asymmetric unit consists of two different kinds of *p*-cresol molecules and all molecules occupy sites of C_1 symmetry in unit cell. In this case factor group selection rules predict 48 lattice vibrations therein 24 rotational modes in the lattice vibrational region (below 150 cm^{-1}). Twelve of them ($6A_g + 6B_g$) are expected to be Raman active (Table 3). The above expectations are partially fulfilled for the *p*-cresol. Four bands and five shoulders are observed in the Raman spectrum of PC below 150 cm^{-1}. Also partial fulfillments of the selection rules for the C_{2h}^5 aromatic organic crystals (naphthalene,

naphthalene-d_8, anthracene, p-dichlorobenzene, p-dibromobenzene and biphenyl) in the lattice vibrations region in polarized Raman spectra were reported by Ito et al. [33]. They noticed that in some studied crystals number of bands derived from rotational modes and observed in the spectrum is less than predicted ones by group theory and they supposed that this is due to small $A_g - B_g$ splitting. In such case some lines observed in the Raman spectrum actually consist of two lines of A_g and B_g species having nearly the same frequency.

The crystal structure of *p*-cresol saturated with Xe has been unknown so far, only suggestions for this structure are currently available in the literature [19,20]. According to them we can assume that the PCXe crystal could crystallize in the $R\bar{3}$ space group similarly as β-hydrochinon saturated with Xe [13,37]. Out of all possible site in the primitive unit cell of this space group only site of C_1 symmetry can be occupied by *p*-cresol molecules in the *p*-cresol crystal saturated with Xe gas. Multiplicity of this site is equal to six [38]. It means that six molecules of *p*-cresol should there are in the unit cell. In such case, taking into account the possibility of vibrational coupling between the six p-cresol molecules in the unit cell, each of the three rotational vibrations of species *A* in the site group might split into six components of species A_g, E_g, A_u and E_u in the factor group. The results of factor group analysis for lattice modes of *p*-cresol crystal saturated with Xe under the above assumptions ($R\bar{3} = C_{3i}^2 = S_6^2$ space group, Z = 6, site symmetry of C_1) are collected in Table 4. From this Table it is seen that six bands due to the rotational modes should be active in the lattice vibrational region of Raman spectrum of PCXe. Three of them correspond to A_g species and the remaining three are of E_g symmetry. In the Raman spectrum of *p*-cresol crystal saturated with Xe gas in the lattice vibrational region three bands and three shoulders due to the rotational vibrations are present (Table 1).

On cooling PCXe sample the bands due to the rotational modes shift to higher wavenumbers. Number of these bands does not change and only some of them become better resolved and defined (Table S1, Fig. S3). It shows that our predictions based on the selection rules for the crystal at room temperature remain in effect for the crystal at lower temperatures.

Summarizing up what has been said so far we can state the following. The selection rules for the lattice vibrational region are different for both crystals. Twelve rotational vibrations ($6A_g + 6B_g$) one can expect in the lattice vibrational region of Raman spectrum of PC crystal and six rotational vibrations ($3A_g + 3E_g$) should be active in lattice vibrational region of Raman spectrum of PCXe. Our experimental results are in agreement with the selection rules developed above. In the Raman spectrum of *p*-cresol four bands and five

shoulders are observed. In the Raman spectrum of *p*-cresol saturated with Xe gas three bands and three shoulders in the lattice vibrational region were identified. In the low temperature spectra six bands are observed in this region (Fig. S3). These observations confirm that the Xe atoms were captured by *p*-cresol and that crystal structure of resulting unstable (under normal conditions) *p*-cresol - Xe clathrate is as established by Selent et al. [22] for the xenon clathrates of *o*- and *m*-fluorophenols.

3.2 Character of PCXe clathrate

Our results presented here are in line with previously published data and suggestions on *p*-cresol – Xe complexation as well as with predictions for similar clathrate systems. It is very well known that phenol and different substituted phenols are able to form complexes with atoms of noble gases – with Xe in the first [19,20,24]. Expected structural motif of these clathrates are two hexagonal rings of coupled $[\cdots O\text{-}H\cdots O\text{-}]_6$ H-bonds and the guest placed between them [13,19,20,24].

Table 2 shows positions and intensity ratios of doublet considered by us in this report as the indicator of the O-H···O bonds strength. These data for the Xe clathrates of hydroquinone (HQXe) and *p*-cresol (PCXe) predict weaker O-H···O bonds in the case of *p*-cresol (Table 2). This conclusion is in very good agreement with relative positions of the bands due to the O-H stretching vibrations: νOH(PCXe) = 3224 cm^{-1} and νOH(HQXe) = 3160 cm^{-1} (Table 1 and [12], respectively), because the higher νOH for PCXe reflects its weaker H-bonds [35].

To estimate the R(O···O) distance in the H-bonds of PCXe clathrate we use the procedure previously applied by us for estimation of temperature induced variation of the R(O···O) distance in the H-bonds of the HQXe clathrate [13]. It is based on the general Novak relationship between the νOH stretching frequency and R(O···O) distance in different chemical compounds containing O-H···O hydrogen bonds [35] and on assumption that the steepness, $\frac{\Delta\nu}{\Delta R(O\cdots O)}$, of the νOH vs. R(O···O) curve for 2.65 ≤ R(O···O) ≤ 2.75 Å range is equal to ~ 2500 $cm^{-1}Å^{-1}$ [13]. Taking above value of the νOH vs. R(O···O) curve steepness and the νOH stretching frequency difference: ΔνOH = νOH(PCXe) - νOH(HQXe) = 3224 – 3160 = 64 cm^{-1} (from Table 1 in this work and from [12], respectively) we predict $\Delta R(O\cdots O) = R(O\cdots O)_{PCXe} - R(O\cdots O)_{HQXe} \approx 0.03$ Å. Recently we have estimated $R(O\cdots O)_{HQXe} \approx 2.71$ Å at

room temperature [13] and then now we predict $R(O\cdots O)_{PCXe} \approx 2.74$ Å also at room temperature (Table 5).

The HQXe clathrate is stable at room temperature and the Xe release from this complex is observed at about 410 K [13]. The H/D isotopic substitution in the O-H···O hydrogen bonds of HQXe crystal is responsible for about 0.01 Å elongation of the R(O···O) distance and for decreasing the temperature of the Xe escape from 410 K (unsubstituted HQXe) to 375 K in its deuterium substituted analogue (DQXe) [13]. It shows that predicted by us 0.03 Å elongation of the R(O···O) distance in the hexagonal rings of coupled $[\cdots O\text{-}H\cdots O\text{-}]_6$ H-bonds, when β-hydroquinone – Xe clathrate is replaced by its *p*-cresol analogue, should result in the Xe release from PCXe near the room temperature. It is in agreement with earlier observations of the Xe release from this clathrate [19,20,24]. Table 5 and Fig. 2 show correlation between temperature of Xe removal from considered here clathrates (HQXe, DQXe, CPXe) and R(O···O) distance in hydrogen bond rings of the host cages.

Recently, for HQXe clathrate we have found experimental evidence on weak interactions between Xe guest and acidic protons of the cage in hydroquinone host and we have estimated $-\Delta H(Xe\cdots H) > 6.2$ kJ mol^{-1} for each H-bonding-like contact Xe···H-O [13]. In the considered here PCXe clathrate these interactions are expected to be weaker due to bigger size of its cage. It means smaller stabilizing role of Xe in this case (in comparison to the HQXe clathrate).

4. Conclusions

Our results show very high sensitivity of Raman spectra of *p*-cresol on its crystal structure and on its variation due to formation of its clathrate with xenon. The most informative are three regions of these Raman spectra: (i) O-H stretching vibrations despite of low intensity of the bands, (ii) vibrations between 900 and 800 cm^{-1}, (iii) the lattice vibrations. Our results confirm earlier suggestions that the main motif of the clathrate cage are two parallely oriented hexagonal rings of coupled $[\cdots O\text{-}H\cdots O\text{-}]_6$ H-bonds formed due to the interaction between *p*-cresol and xenon. We estimated the O···O distance in these bonds. It is longer than in the corresponding H-bonds in *β*-hydroquinone – Xe clathrate and it explains lower stability of studied here the *p*-cersol – Xe complex (lower temperature of the Xe release).

Acknowledgement

Project partially supported by Wroclaw Centre of Biotechnology, programme The Leading National Research Centre (KNOW) for years 2014-2018.

The Raman spectra were recorded at Institute of Low Temperature and Structure Research of Polish Academy of Sciences, Wrocław. Professor J. Baran is thanked for his help with Raman spectra measurements and for helpful discussion.

References

[1] J. Furtado, F. De Proft, P. Geerlings, The noble gases: How their electronegativity and hardness determines their chemistry**,** J. Phys. Chem. A 119 (2015) 1339–1346.

[2] J. Haner, G.J. Schrobilgen, The chemistry of xenon(IV), Chem. Rev. 115 (2015) 1255−1295.

[3] D.S. Brock, G.J. Schrobilgen, B. Žemva, Noble-Gas Chemistry, in Comprehensive Inorganic Chemistry, ed. by J. Reedijk, K. Poeppelmeier, Oxford, UK, Elsevier, 2013, vol. 1, Chapter 1.25, p. 755.

[4] S.C. Cullen, E.G. Gross, The anesthetic properties of xenon in animals and human beings, with additional observations on krypton, Science 113 (1951) 580−582.

[5] N.P. Franks, W.R. Lieb, Molecular and cellular mechanisms of general anaesthesia, Nature 367 (1994) 607−614.

[6] N.P. Franks, R. Dickinson, S.L.M. de Sousa, C.A. Hall, W.R. Lieb, How does xenon produce anaesthesia?, Nature 396 (1998) 324.

[7] M.D. Krasowski, N.L. Harrison, General anaesthetic actions on ligand-gated ion channels, Cell. Mol. Life Sci. 55 (1999) 1278−1303.

[8] C. III Lynch, J. Baum, R. Tenbrinck, Xenon anesthesia, Anesthesiology 92 (2000) 865−868.

[9] O. Ozgurel, F. Pauzat, J. Pilmé, Y. Ellinger, M.-C. Bacchus-Montabonel, O. Mousis, Protonated ions as systemic trapping agents for noble gases: **f**rom electronic structure to radiative association, J. Chem. Phys. 147 (2017) 134305.

[10] Ch. Sanloup, S.A. Bonev, M. Hochlaf, H.E. Maynard-Casely, Reactivity of xenon with ice at planetary conditions, Phys. Rev. Letters 110 (2013) 265501.

[11] C. Sandorfy, Weak intermolecular associations and anesthesia, Anesthesiology 101 (2004) 1225−1227.

[12] M. Ilczyszyn, M. Selent, M.M. Ilczyszyna, J. Baran, Infrared spectra of β-hydroquinone–xenon crystal. H/D isotope and temperature effects, Vibrational Spectroscopy 55 (2011) 107–114.
[13] M. Ilczyszyn, M. Selent, M.M. Ilczyszyn, Participation of xenon guest in hydrogen bond network of β-hydroquinone crystal, J. Phys. Chem. A 116 (2012) 3206-3214.
[14] D. Gąszowski, M. Ilczyszyn, Does hydrogen bonding to xenon affect its 129Xe NMR chemical shift? Computational study on selected Brønsted acid–xenon complexes, Chem. Phys. Lett. 538 (2012) 29–34.
[15] D. Gąszowski, M. Ilczyszyn, Hydrogen bonding to xenon: A comparison with neon, argon and krypton complexes**,** Chem. Phys. Lett. 556 (2013) 59–64.
[16] D. Gąszowski, M. Ilczyszyn, Nature of Brønsted acid–noble atom contacts: A reevaluation of hydrogen bonding criteria, Int. J. Quant. Chem. 114 (2014) 473–480.
[17] Ł. Wołoszyn, M. Ilczyszyn, M.M. Ilczyszyn, Experimental evidence on interaction between xenon and bovine serum albumin, Spectrochim. Acta A 125 (2014) 449–452.
[18] D. Gąszowski, M. Ilczyszyn, The acid-base character of interactions between xenon and selected carboxylic and sulfonic acids, Chem. Phys. 488-489 (2017) 22−27.
[19] D.D. MacNicol, J.J. McKendrick, D.R. Wilson, Clathrates and molecular inclusion phenomena, Chem. Soc. Rev. 7 (1978) 65–87.
[20] R.M Barrer, V.H. Shanson, Clathration by *para*-substituted phenols, J**.** Chem. Soc., Faraday Trans.1 72 (1976) 2348–2354.
[21] J.A. Ripmeester, Nuclear shielding of trapped xenon obtained by proton-enhanced, magic-angle spinning xenon-129 NMR spectroscopy, J. Am. Chem. Soc. 104 (1982) 289−290.
[22] M. Selent, J. Nyman, J. Roukala, M. Ilczyszyn, R. Oilunkaniemi, P.J. Bygrave, R. Laitinen, J. Jokisaari, G.M. Day, P. Lantto, Clathrate structure determination by combining crystal structure prediction with computational and experimental ^{129}Xe NMR spectroscopy, Chem. Eur. J. 23 (2017) 5258–5269**.**
[23] Q. Cao, N. Andrijchenko, A. Ermilov, M. Räsänen, A. Nemukhin, L. Khriachtchev, Interaction of aromatic compounds with xenon: Spectroscopic and computational characterization for the cases of *p*-cresol and toluene, J. Phys. Chem. A 119 (2015) 2587-2593**.**
[24] A.M. Trofimov, Yu.N. Kazankin, Klatratnye soedinenia π-krezola s blagorodnymi gazami (russ), Radiokhimiya 7, 1965, 288–292.

[25] S.-P. Kang, H. Lee, Equilibrium dissociation pressures for *p*-cresol + methane and *p*-cresol + nitrogen clathrates at temperatures above the normal melting temperature of *p*-cresol, J. Chem. Eng. Data 42 (1997) 467–469.

[26] R. Flacau, S. Desgreniers, J.S. Tse, Electron density topology of cubic structure I Xe clathrate hydrate at high pressure, J. Chem. Phys. 129 (2008) 244507.

[27] S. Takeya, A. Hachikubo, Structure and density comparison of noble gas hydrates encapsulating xenon, krypton and argon, Chem. Phys. Chem. 20 (2019) 2518–2524.

[28] J.-P. Torré, R. Coupan, M. Chabod, E. Péré, S. Labat, A. Khoukh, R. Brown, J.-M. Sotiropoulos, H. Gornitzka, CO_2−hydroquinone clathrate: Synthesis, purification, characterization and crystal structure, Cryst. Growth Des. 16 (2016) 5330−5338.

[29] R. Coupan, E. Péré, Ch. Dicharry, and J.-P. Torré, New insights on gas hydroquinone clathrates using in **s**itu Raman **s**pectroscopy: Formation/dissociation mechanisms, kinetics, and capture **s**electivity, J. Phys. Chem. A 121 (2017) 5450−5458.

[30] V.F. Rozsa, T.A. Strobel, Triple guest occupancy and negative compressibility in hydrogen-loaded β‑hydroquinone clathrate, J. Phys. Chem. Lett. 5 (2014) 1880−1884.

[31] H. Takeuchi, N. Watanabe, I. Harada, Vibrational spectra and normal coordinate analysis of *p*-cresol and its deuterated analogs, Spectrochim. Acta A 44 (1988) 746–741.

[32] M.N. Siamwiza, R.C. Lord, M.C. Chen, T. Takamatsu, I. Harada, H. Matsuura, T. Shimanouchi, Interpretation of the doublet at 850 and 830 cm-1 in the Raman spectra of tyrosyl residues in proteins and certain model compounds, Biochemistry 14 (1975) 4870–4876.

[33] M. Ito, M. Suzuki, T. Yokoyama, Raman active lattice vibrations of organic crystals, in Excitons, Magnons and Phonons in Molecular Crystals, ed. by A.B. Zahlan, London Cambridge UP, 1968, pp. 1-29.

[34] E. Batisai, V.J. Smith, S.A. Bourne, N.B. Báthori, Solid state structures of *p*-cresol revisited, Cryst. Eng. Comm. 17 (2015) 5134–5138.

[35] A. Novak, Hydrogen bonding in **s**olids. Correlation of spectroscopic and crystallographic data, Struct. Bonding (Berlin), 18, 1974, 177−216.

[36] P.C. Bois, Structure du *p*-crésol á basse température, Acta Cryst. B 26 (1970) 2086.

[37] T. Birchall, Ch.S.Frampton, G.J. Schrobilgen, J. Valsdóttier, β-Hydroquinone xenon clathrate, Acta Cryst. C45, 1989, 944–946.

[38] G.Turrell, Infrared and Raman spectra of crystals, Academic Press, London and New York, 1972, p. 99.

Figure captions

Fig 1. Raman spectra of *p*-cresol (PC; red) and *p*-cresol – Xe (PCXe; blue) samples in the selected regions: a) 3625 – 2250 cm^{-1}; b) 2000 – 1100 cm^{-1}; c) 1100 – 250 cm^{-1}; d) 250 – 10 cm^{-1}.

Fig. 2. Correlation between temperature of Xe release from hydroquinone – Xe (HQXe), deuterium substituted hydroquinone – Xe (DQXe) and *p*-cresol – Xe (PCXe) clathrates and R(O···O) distances in hydrogen bond rings of the host cages (the temperature 293 K was assumed for PCXe).

Figure(s)

Click here to download high resolution image

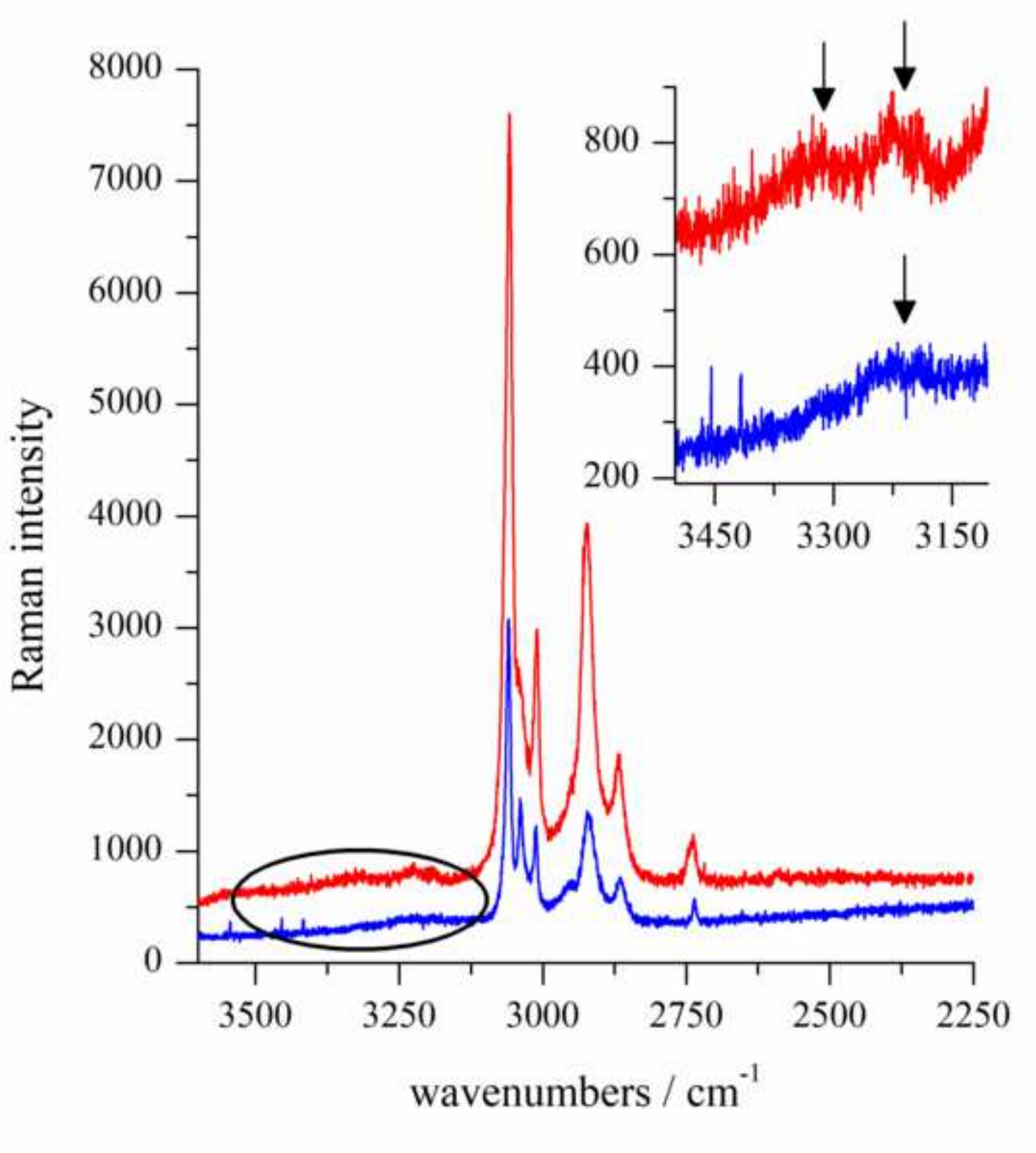

Figure(s)

Click here to download high resolution image

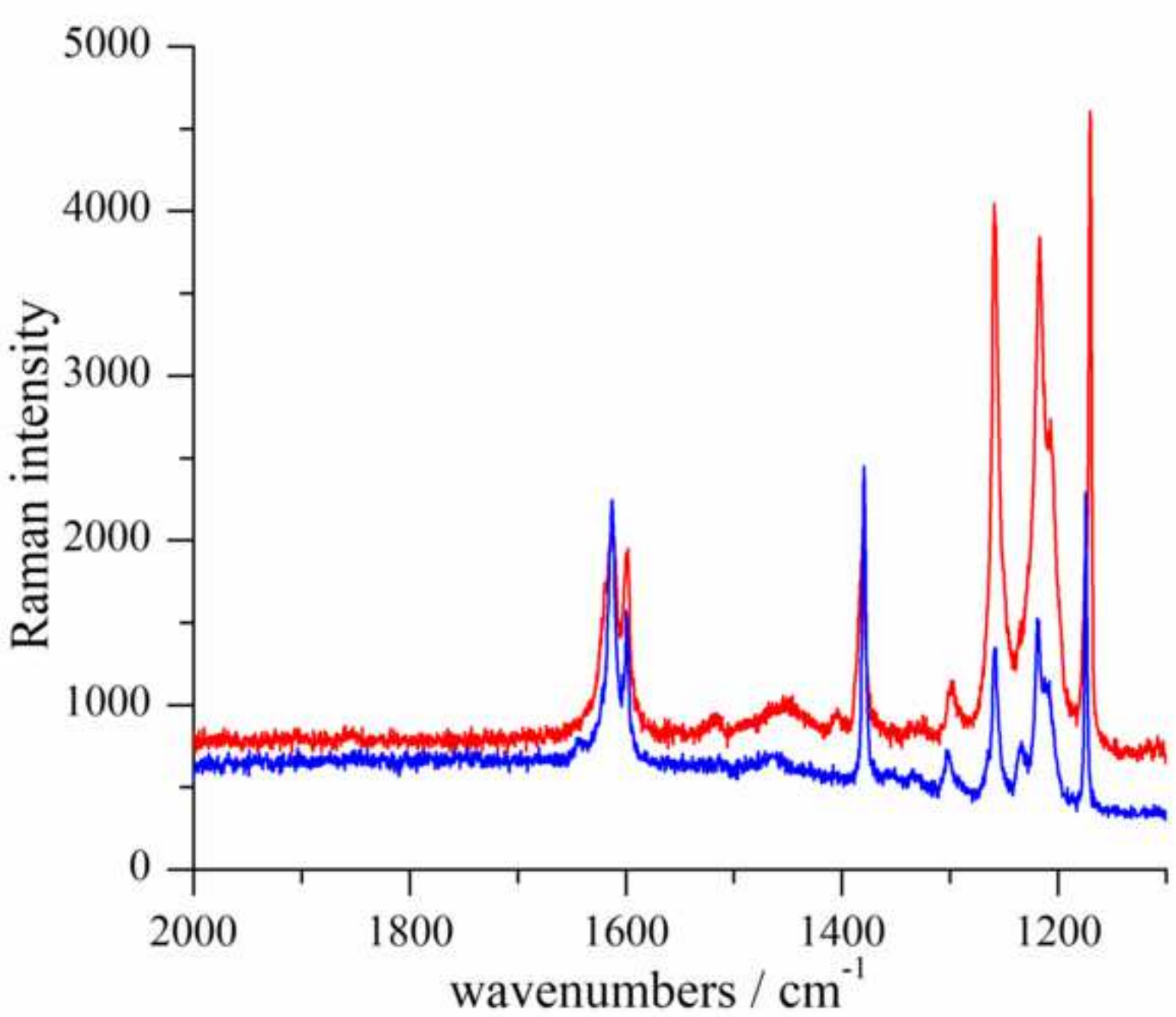

Figure(s)

Click here to download high resolution image

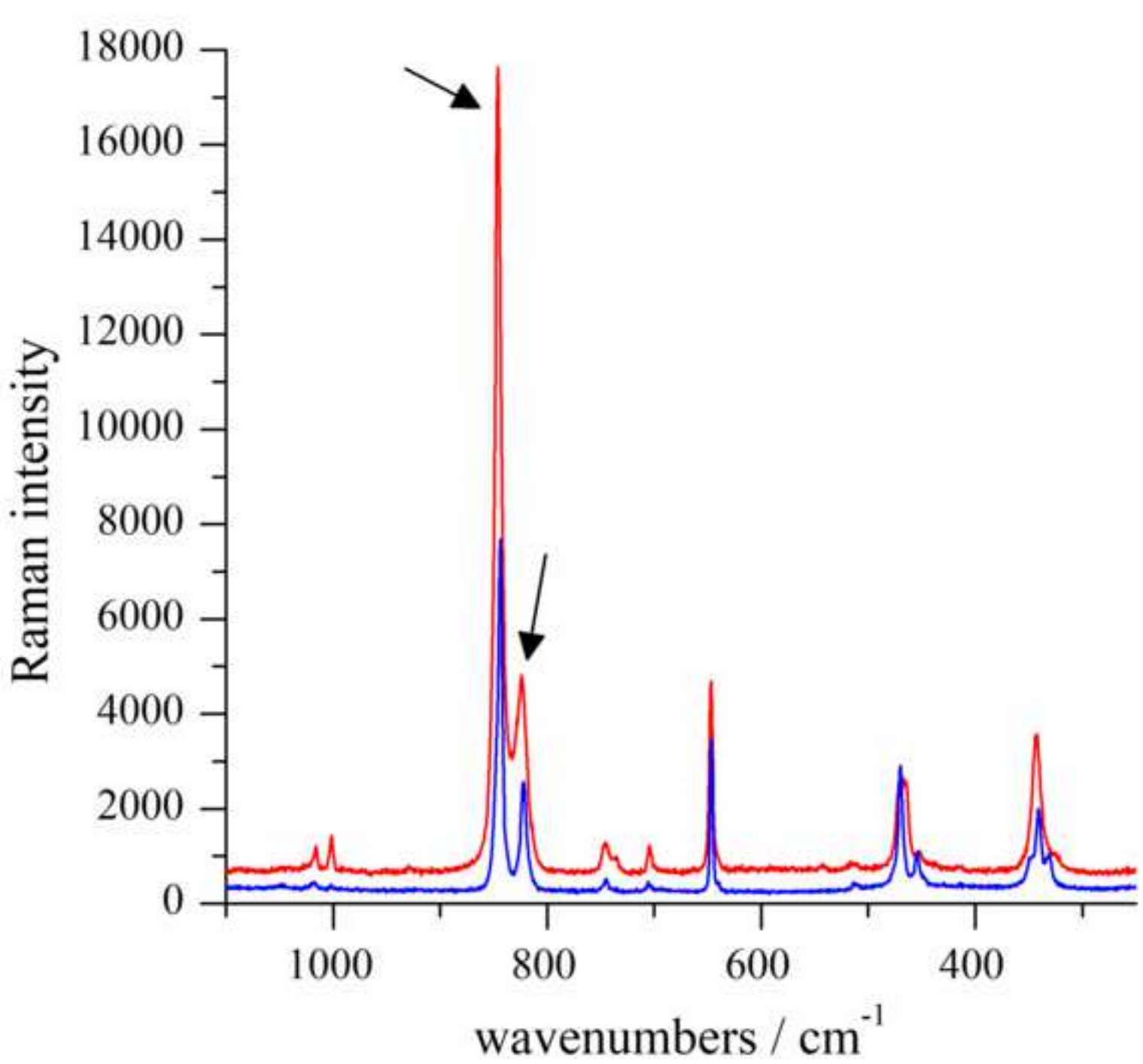

Figure(s)

Click here to download high resolution image

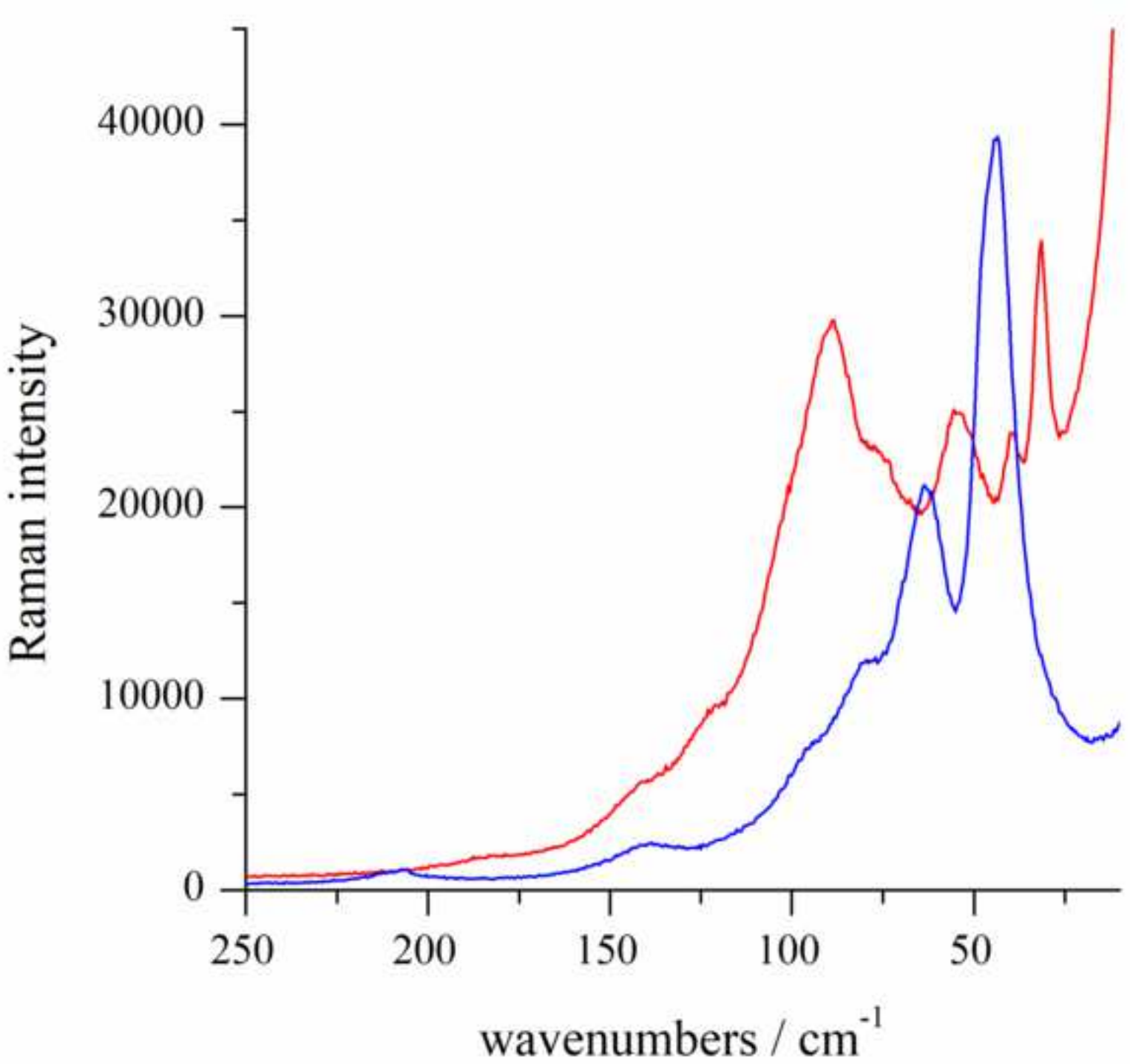

Figure(s)

Click here to download high resolution image

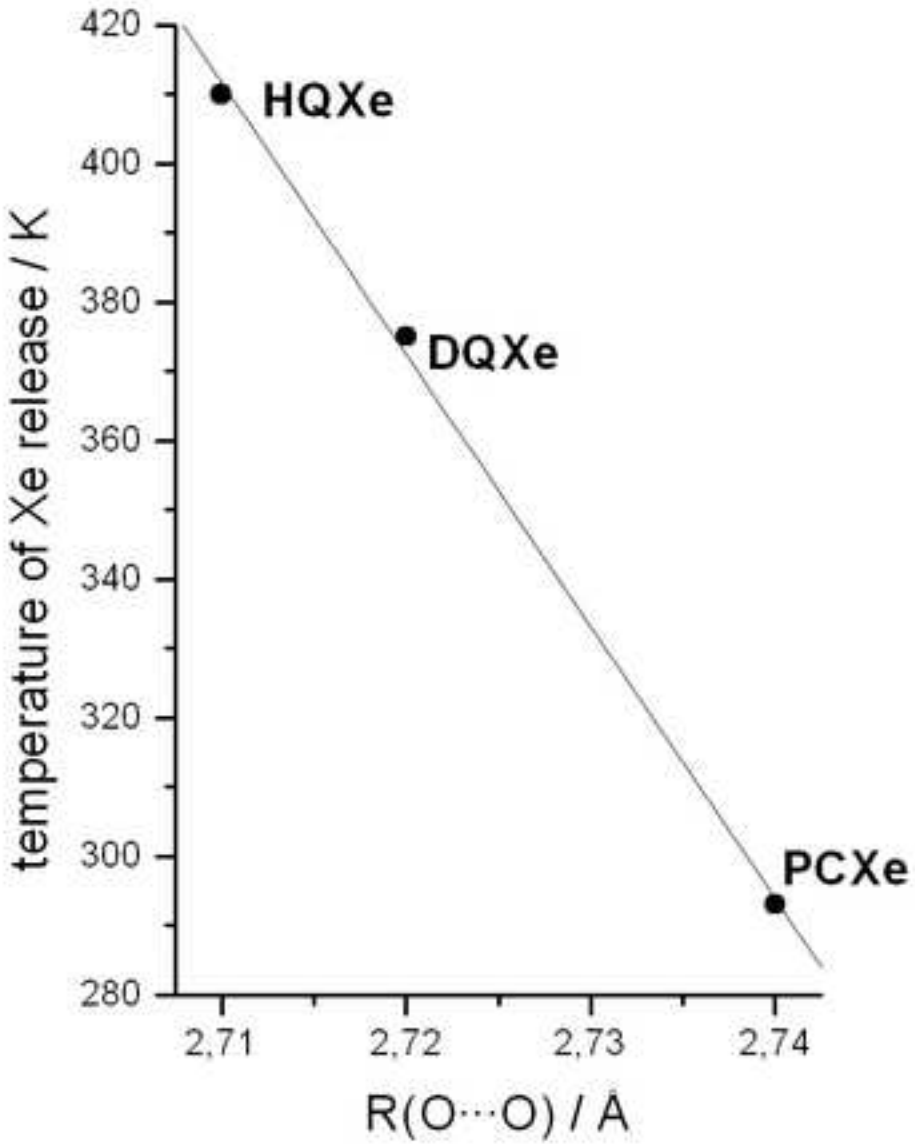

Table(s)

Table 1. Wavenumbers of the bands observed in Raman spectra of *p*-cresol (PC) and *p*-cresol – Xe (PCXe) samples measured at room temperature.

Raman spectra		Tentative assignments
p-cresol (PC)	*p*-cresol +Xe (PCXe)	
3320 (98)[a]		νOH
3224 (26)	3224 (11)	νOH
3058 (223)	3060 (79)	ν_2 (νCH)
3041 (75, sh)	3039 (36)	ν_{20ab} (νCH)
3010 (89)	3012 (30)	ν_{7b}(νCH)
2950 (45, sh)	2950 (18, sh)	$\nu_a CH_3$
2923 (114)	2921 (34)	$\nu_s CH_3$
2867 (53)	2864 (19)	$\nu_a CH_3$
2742 (29, sh)		
2738 (32)	2735 (14)	
1618 (50, sh)	1621 (28, sh)	
1613 (53)	1612 (57)	ν_{8a} (νCC)
1599 (56)	1599 (40)	ν_{8b} (νCC)
1517 (26)	1516 (17)	ν_{19a} (νCC+ δCH)
1451 (29)	1461 b (17)	$\delta_a CH_3$
1404 (28)		ν_{19b} (νCC+ δCH)
1383 (52, sh)		
1380 (58)	1379 (63)	$\delta_s CH_3$
	1352 (15)	
1329 (25)	1333 (15)	ν_3 (δCH + νCC)
1298 (32)	1301 (33)	ν_{14} (νCC+ δCH)
1258 (113)	1258 (34)	νC-O
	1234 (19)	
	1218 (38)	
1207 (78)	1210 (28)	νCCH_3, ν_{7a} (νCH)
1175 (59)	1174 (59)	ν_{9a} (δCH)
1170 (137)		
1015 (36)	1018 (11)	ν_{18a} (δCH), νCC+γCCC
1001 (42)	1002 (9)	ρCH_3
	847 (83, sh)	
846 (521)	844 (196)	ν_1+2ν_{16a}
824 (139)	821 (66)	ν_1+2ν_{16a}
745 (38)	745 (13)	νCCH_3+ νCO
734 (29)		
703 (36)	705 (12)	ν_4 (πCO+πCCH+πCH)
646 (138)	646 (88)	ν_{6b} (γCCC)
	639 (11, sh)	
542 (24)		
513 (24)	513 (11)	ν_{16b} (πCO+πCCH_3)
	509 (10)	
473 (13)		
468 (77)	469 (74)	ν_{6a} (γCCC)
452 (32)	453 (28)	

	448 (14, sh)	
414 (24)		ν_{16a} (τCC)
	347 (25, sh)	
342 (105)	340 (51)	ν_5 (δCH), $\delta CCH_3+\delta CO$
326 (31, sh)	331 (27)	$\pi CCH_3+\pi CO+\tau CC$
	206 (24)	τCO
141 (167, sh)	138 (62)	Rotational mode
120 (283, sh)		Rotational mode
100 (615, sh)	93 (197, sh)	Rotational mode
91(848, sh)		Rotational mode
88 (875)		Rotational mode
77 (680, sh)	78 (302, sh)	Rotational mode
	62 (534)	Rotational mode
54 (733)	48 (800, sh)	Rotational mode
	44 (1000)	Rotational mode
39 (707)		Rotational mode
31 (1000)		Rotational mode

[a] In brackets, the relative intensities of the bands regarding to the most intense band in the spectrum are given. The intensity equal to 1000 was assumed for the most intense band in the spectrum

Table 2. Frequencies (cm^{-1}) and intensity ratios of the Fermi doublet in Raman spectra of *p*-cresol (PC) and *p*-cresol – Xe (PCXe) crystals and in infrared spectrum of *β*-hydroquinone – Xe crystal (HQXe) [12].

Crystal	Frequency of component 1 (cm^{-1})	Frequency of component 2 (cm^{-1})	1:2 Intensity ratio
PC	846	824	11:3
PCXe	844	822	9:3
HQXe	852	832	4:3

Table 3. Symmetry species of lattice modes of *p*-cresol crystal.

Factor group C_{2h}	Acoustic modes	Rotational modes	Translational modes	Raman and IR activity
A_g		6	6	α_{xx}, α_{yy}, α_{zz}, α_{xy}
B_g		6	6	α_{xz}, α_{yz}
A_u	1	6	5	*z*
B_u	2	6	4	*x,y*

Table 4. Symmetry species of lattice modes of *p*-cresol – Xe crystal (determined under assumption: $R\bar{3}$, Z = 6, site symmetry C_1).

Factor group S_6 (C_{3i})	Acoustic modes	Rotational modes	Translational modes	Raman and IR activity
A_g		3	3	$\alpha_{xx} + \alpha_{yy}$, α_{zz}
E_g		3	3	$(\alpha_{xx} - \alpha_{yy}, \alpha_{xy})$, $(\alpha_{yz}, \alpha_{zx})$
A_u	1	3	2	*z*
E_u	1	3	2	*x, y*

Table 5. Distances between oxygen atoms [R(OO)] in the hexagonal rings of $[\cdots O\text{-}H\cdots O\text{-}]_6$ bonds in xenon clathrates of hydroquinone (HQXe), deuterium substituted hydroquinone (DQXe), *p*-cresol (PCXe) and temperature release of Xe from these complexes (this work and ref. [13]).

Clathrate	R(OO) (Å)	Temperature of Xe release (K)
HQXe	2,71	410
DQXe	2,72	375
PCXe	2,74	ca. 293